



Surface irregularities in titanium marine parts formed by the particulate injection moulding process

Paul D. Ewart¹, Kieran Mangan¹, Seokyoung Ahn², Lukas Capek³

- 1) Centre for Engineering and Industrial Design, paul.ewart@wintec.ac.nz, kieman17@student.wintec.ac.nz, Waikato Institute of Technology, 51 Akoranga Road, Rotokauri Campus, Hamilton 3240, New Zealand
- 2) Mechanical Engineering, sahn@pusan.ac.kr, Pusan National University, 2, Busandaehak-ro 63beon-gil, Geumjeong-gu, Busan, 46241, Republic of Korea
- 3) Department of Technologies and Structures, lukas.capek@tul.cz, Technical University of Liberec (TUL), Studentská 2, Liberec 1, 461 17 Czech Republic

Keywords

Particulate Injection Moulding, Polymer, Solid Modelling, Segregation, Titanium Metal

Abstract

In this study, a structural hold down component was designed and produced using the particulate injection moulding (PIM) process. The material of choice was titanium due not only to the material properties but also due to the desire to create custom-made components for a state-of-the-art marine vessel, Earthrace 2.

On removal from the mould, the green parts were seen to have an irregular surface on the top face. Known as surface bloom, it can be seen during moulding of single-phase commodity polymers as a result of changes in the polymer density, due to shear stresses and irregularities of turbulent flow.

Literature suggests the surface bloom is a result of a separation between the two phases, but the preliminary findings show little evidence of this within the sectioned profile. The sintered parts were sectioned, and inspection of the surfaces was done using metallographic techniques. The use of CAD models enabled the defect to be modelled and the models provided a more likely scenario. It was further confirmed that there were no through part defects present and although the surface irregularities were caused by separation of the two-phases, the effect was restricted to the outer surface of the parts.

1 Introduction

High-alloy steels with addition of > 10 % chromium are known as stainless steels [1] and due to their increased strength and oxidation resistance are used for food production equipment, in the chemical industry and in marine environments. A problem within some marine environments is that corrosion still occurs. The corrosion still occurs despite the alloying content because of high mechanical stress, a result of high loading. This is particularly seen in structural applications and load points. While this may be acceptable within industries such as commercial fishing and container transportation, it is not desirable in luxury vessels or high-performance sports vessels. To eliminate the effects of stress on these components, materials with greater oxidation resistance are recommended, one of which is titanium metal. Not only does titanium metal have greater oxidation resistance than marine alloyed chromium steels, it also has lower density and higher yield strength, which enable lower weight and lower material utilisation.

In this study, a structural hold down component was designed and produced using the particulate injection moulding (PIM) process. Part dimensions with an envelope of Φ 80 mm x 30 mm with an average thickness of 4 mm. The material of choice was titanium due not only to the material properties

Digital Object Identifier: <http://dx.doi.org/10.21935/tls.v3i1.139>

www.lightweight-structures.de

This is an open access article under the CC BY 4.0 license (<http://creativecommons.org/licenses/by/4.0/>)

mentioned previously but also due to the desire to create custom-made components for a state-of-the-art marine vessel, Earthrace 2.

The component was produced using the particulate injection moulding (PIM) process [2]. This fabrication technique was used due to several efficiencies offered by the process. It supports materials sustainability of the powder metallurgy approach by using only the volume of metal required to create the necessary part geometries (material utilisation) [3]. It has high reproducibility, which is desirable for high volume of parts, it produces isotropic material properties and where necessary can be used to provide unique alloys not possible from wrought material [4].

The original design was modified to better utilise the titanium properties and, using a polymer mould tool, green parts were produced with green machining, used to mark the parts with logos and identifiers and apply final features. The tests were never completed, as the break was always the lifting shackle used to connect mounts to the universal testing instrument. The load shackles had working capacity six times that required for the mounts. To this end, the mounts were redesigned and a material saving of some 40 % was realised. The new components therefore having a thinner wall section and a corresponding reduction in loading capability is expected.

An unexpected result of reducing the wall thickness was an irregularity seen on the upper surface of the mount. The irregular surface appeared in no particular order during moulding and was seen to stay in the part through all processing steps (Figure 1 b)). The irregular surface was seen in 10 of the 28 parts that were moulded. The concern being whether the visual phenomenon would affect the microstructure and/or mechanical properties of the part in use. A similar visual can be seen during plastic moulding of single-phase commodity polymers and is known as surface bloom [5]. It is proven to be a result of changes in the polymer density and separation of components due to shear stresses, incompatibility and irregularities of turbulent flow.

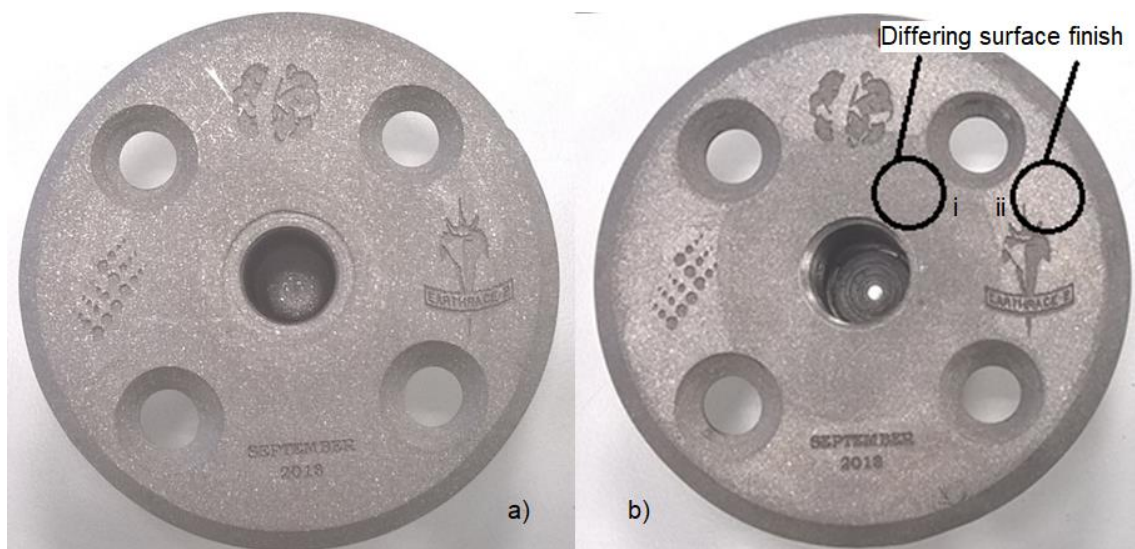


Figure 1: The sintered titanium part a), and b) the part with surface irregularities (i & ii) on the top face

The PIM process uses a two-phase (polymer carrier and the titanium particles) metallic blend or feedstock that behaves in a different manner to a polymer [6]. The literature suggests the phenomenon, similar to surface bloom, can be a result of a separation between the two phases [7]. Regardless of the mechanism creating the irregularities on the top face of the part, they are processing defects. Therefore, the issue that needs to be resolved is how it will be rectified. If it is a structural defect, it is critical, the parts produced will be scrapped and the part will require a redesign, flow optimisation and retooling. If it is a cosmetic defect, it is not so critical and a surface treatment may suffice [8].

The parts are investigated following the experimental procedure set out below, with mechanical testing, combined sampling and optical imaging showing the effect in greater detail.

2 Experimental design

2.1 Materials

The tooling seen in Figure 2 was produced using a modular approach from polyamide and aluminium with a conventional sprue made of tool steel. The components were moulded using a PolyMIM titanium feedstock with a water soluble binder (PolyMIM Ti grade 2, oversize factor 1.151 ave., $\sigma_y \geq 270$ MPa, $\rho \geq 4.3$ g/cm³, particle size ≤ 45 μ m) supplied by PGE Injection Moulding Ltd (PGE).

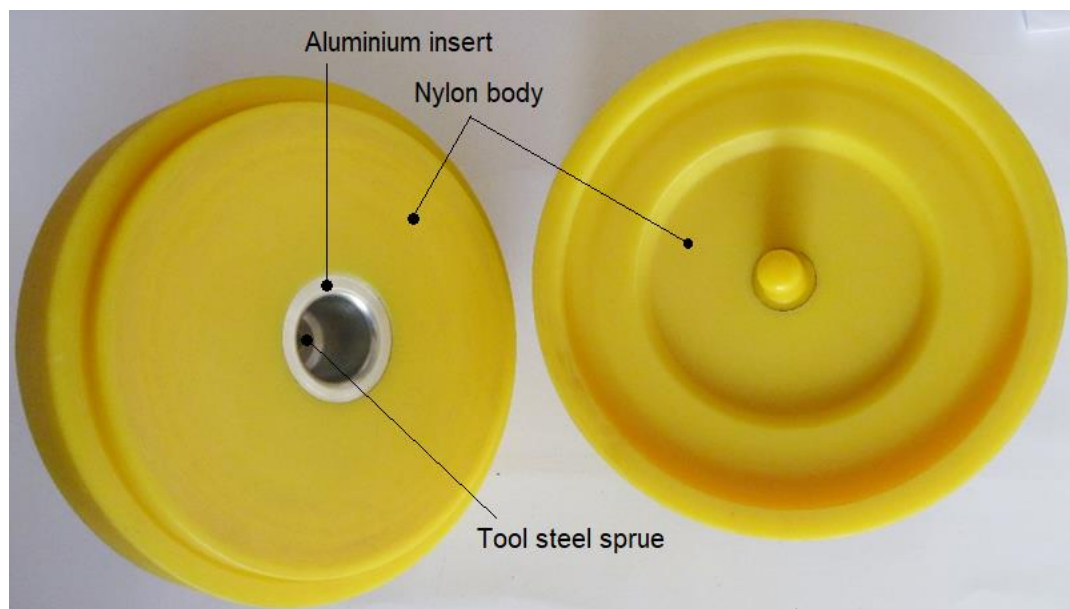


Figure 2: Composite tool insert produced using polyamide (nylon), aluminium and tool steel, suitable for production run < 100 parts

The cross section of the tool is shown in Figure 3 with the aluminium and steel parts connected to the fixed plate.

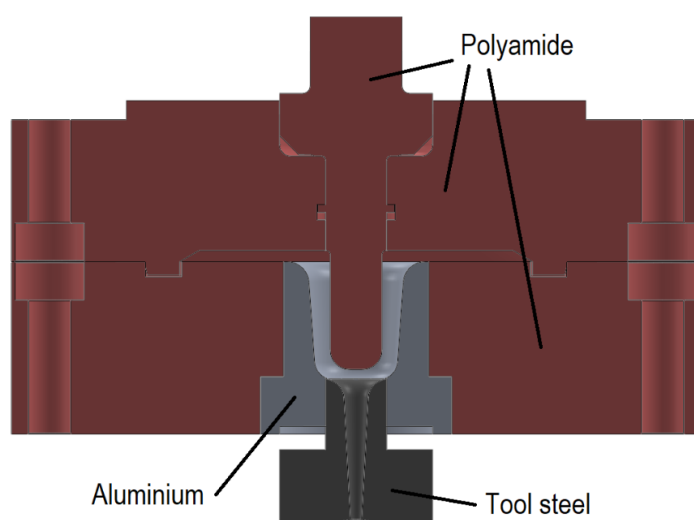


Figure 3: The cross section of the composite tool

2.2 Processing

The moulding was done with a barrel temperature of 185 °C using the Arburg 170 injection moulding machine with a 38 mm diameter barrel and complementary screw to produce green parts. Solution treatment was done in the PGE custom debinding unit using a RO treated water solution to remove the soluble binder component. Drying was done in a Contherm convective drying oven to drive away all moisture. Green machining was done using a manual lathe, pedestal drill and 80 W laser engraver.

Thermal treatment and sintering was done using the Elnik MIM3002 furnace (cold wall, all molybdenum hot zone and retort) by CTCV Materials, Portugal.

Mechanical testing was done using the Lloyd 30LR universal testing instrument in a custom setup to replicate the parts in use. A proving strength test was done to ensure the parts were capable of withstanding a working load of 500 kg. The parts were loaded to 20 kN, which corresponds to a factor of safety of > 4.

Mechanical testing was also carried out using the Pasco ME8237 materials testing equipment and the three-point bend apparatus. This was used to compare the strength of the parts radially and transversely to the line seen between the regular and irregular surfaces.

Analysis sample preparation was done using the IsoMet 1000 sectioning saw, Metaserv 250 polisher and vector 250 power head. The microstructure images were taken with the Buehler ViewMet inverted microscope with uEye digital 1460LE-C camera.

2.3 Method

The green parts were moulded at a melt temperature of ~ 180 °C and an 80 MPa injection pressure. A six-step shot progression was done to determine the shot size and bring the tool surfaces to a steady state temperature. Thirty parts were moulded and a green machining process followed solution treatment. Extra features can be included in the moulding process, but require complex tooling. The increased cost is only viable with higher production volumes.

The green parts were solution treated at 60 °C in water that had been through reverse osmosis to purify it and reduce the level of dissolved solids. The treatment was run for 36 h to remove about 50 % of the total binder content to reduce the green part mass by ~ 7 %.

Green machining was done to remove moulding blemishes and add more part features (countersunk holes) needed for the hold down parts. Laser marking (manufacturer and end user logos), weighing and dimensional checks as a means of quality control were also done, after debinding had been completed.

Final consolidation was achieved through a thermal treatment optimised for the titanium feedstock and based on part size and section thickness. There are two stages to the consolidation: thermal debinding to remove all remaining binder and the sintering to coalesce the titanium [4]. The MIM furnace allows both stages to be completed in the one thermal profile.

The thermal profile consisted of a series of heating ramps and isothermal holds (dwell) to remove the residual binder and enable coalescence of the titanium particles. The thermal profile ramped from room temperature to 250 °C, this enabled the heat to soak through the parts. At this point, the furnace atmosphere was changed to oxygen, carbon, hydrogen and nitrogen free, with partial pressure to encourage removal of the thermoplastic binder through the elemental gradient. The thermoplastic binder system was composed of those very elementals and so the atmosphere was continually replenished during the temperature ramp until all the elemental residuals were removed. The thermal profile followed the ramp-dwell process until the binder was totally removed from the part somewhere near 550 °C.

With debinding complete, the atmosphere was maintained with only temperature changes, enabling the sintering process and particle coalescence to consolidate the part. In this work, a final sinter temperature of 1340 °C was used with a dwell time of 150 minutes. After this step, the temperature was returned to ambient before the furnace was opened. The total thermal cycle was about 18 hours with a further cooling time of 6 hours.

Investigations into the nature and effects of the surface irregularities were done. The parts were sectioned and samples ground and polished using the Buehler kit. Samples were inspected using the light microscope, as found, after polishing, and after grit blasting.

The parts were also sectioned to obtain samples cut in the manner seen in Figure 4. Samples were 5.0 mm x 4.6 mm x 25.0 mm (W x D x H) and were cut to span 20 mm of the three-point bend anvils, Figure 4. The samples were loaded to failure and the results for the perpendicular orientations were compared.

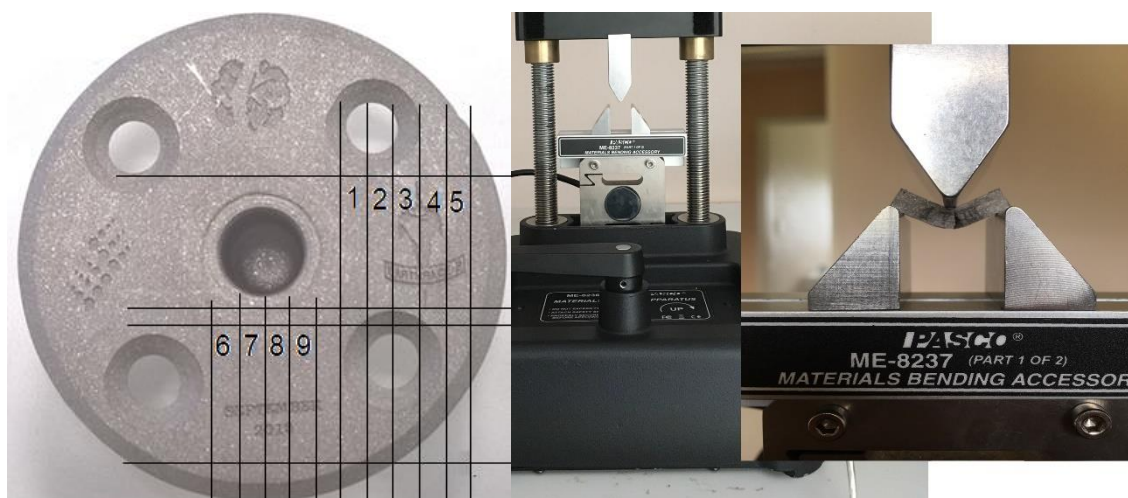


Figure 4: Samples (1 to 10) cut from the sintered part were used in the three-point bend test

The parts were also mechanically load tested by proof loading them in tension at four times the required working load. The load was 20.0 kN with a pre-load of 0.1 kN and a head speed of 100 mm/min. Following this, a loading of 0.1 to 20.0 kN with a cycle time of 30 s was done for a total of 100 cycles.

Once the nature of the defects was ascertained, a solution is presented that will ensure the parts are fit for purpose.

3 Results and discussion

3.1 Inspection of the sintered parts

The regular surface was that with the greatest area of coverage on the parts. Figure 5 shows magnified images of the sintered part surfaces, irregular (Figure 1 b i) and regular (Figure 1 b ii). While particle counts are an often selected means to objectively evaluate disparity over a given area, the equipment available in this work was not suitable for this. The irregular surface finish as seen on the top face of the part is considered a processing defect. It is the nature of the defect that is being investigated. If the defect is seen throughout the part's cross section, it is a structural defect and may have a critical influence on the mechanical properties and the part would require a redesign, mould flow optimisation and retooling. As a cosmetic defect, it would not affect structural integrity and so a surface treatment may suffice as a solution. There are many processes in use to improve the surface of [9], however, there needs to be consideration of cost and time frame for commercial applications.

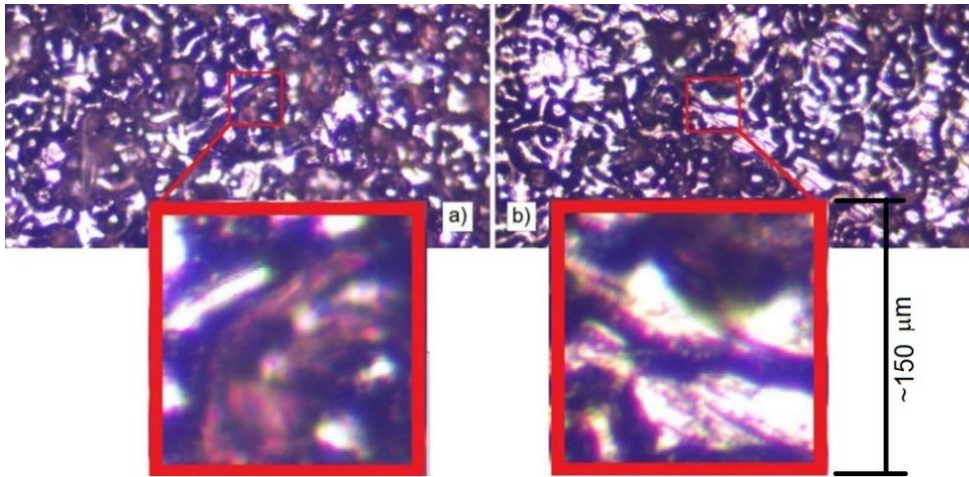


Figure 5: Optical image of sintered surface of titanium part, a) inner surface (i) and b) outer surface (ii)

All 10 parts with the visual surface irregularity were inspected and no discernible difference was seen between them. A difference might indicate the irregularities were due to different mechanisms, such as thermal stresses, mechanical abrasion or density distribution. A sample with an average area of irregularity was used for subsequent analysis. When inspected using the optical microscope, it was seen that the inner surface (Figure 5 a) i) has less particles than the outer surface (Figure 5 b) ii). It was considered that this difference in particle distribution may be creating a visual effect. What it did not show, however, was whether this particle deficiency extended through the part's cross section. To address this, the part was sectioned and showed no defects to indicate separation through the part. The cross section shown in Figure 6 a) confirmed the irregularity with fewer particles at the surface, compared to the cross section depicted in Figure 6 b) with regular particle packing, does not visibly extend beyond the surface of the part.

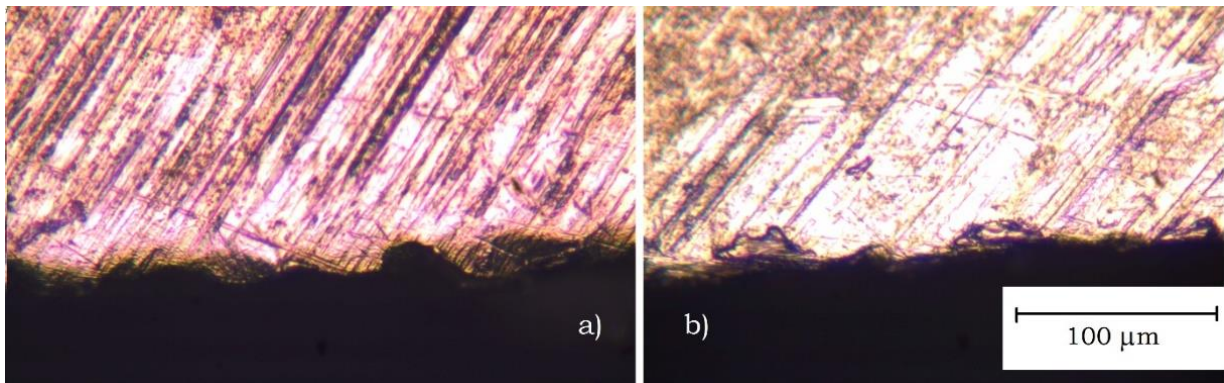


Figure 6: The sectioned parts are seen here as a) irregular surface and b) regular surface

3.2 Analysis of the defect

These surface differences can be attributed to the slip phenomena, as seen here in Figure 7, where binder-rich slip bands can form. As seen in Figure 7, the binder-rich layer at the wall surface is thicker than that of the slip bands within the bulk flow [10]. These differences can be accounted for by considering the blend ratio of particles to binder. It is established that a volume fraction of about 0.63 is typical for 45 μm particles. There are number of variables to be considered such as the binder components, the processing temperature, the geometry of the part and geometry changes the flow front is subjected to. These variables can be addressed with flow properties of the feedstock and the stress-strain relation through viscosity.

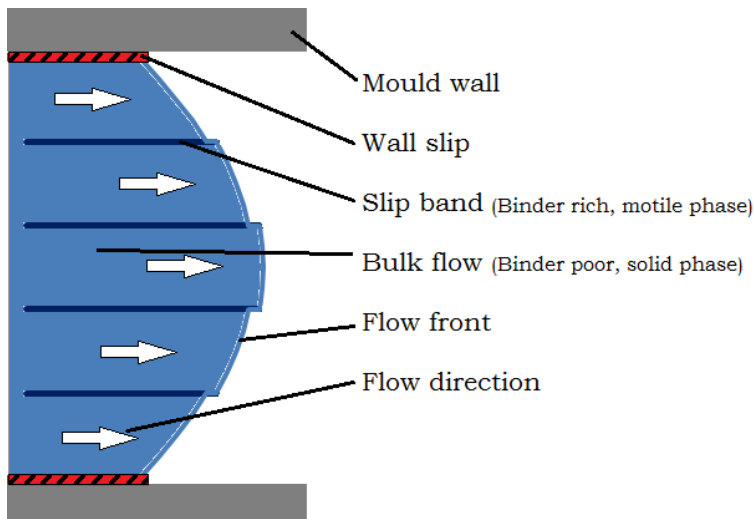


Figure 7: Slip layers forming due to shear and heat sensitivities during moulding [11]

Two material properties that are considered to influence the moulding behaviour in this case are thermal expansion of the feedstock and thermal conductivity of the tooling. The feedstock effect will be seen where temperature variations produce volume change in the thermoplastic binder, increasing the likelihood of separation as the optimised ratio is only realised for a given temperature. The tooling effect will be exacerbated by the composite tooling whereby the thermal conductivity of the mould wall changes as the materials changes, as seen in Figure 2.

3.3 Modelling the defect

Solid modelling was used to produce a visual representation of what was interpreted in the micrograph in Figure 8. The difference in surface particle distribution was replicated based on a spherical particle model at ~ 93 % consolidation using 2D modelling and shown as Figure 8.

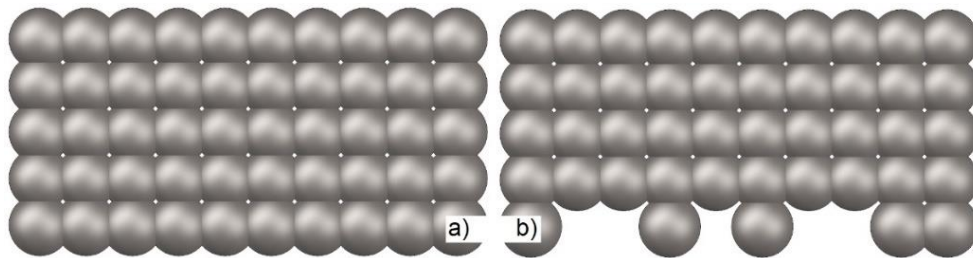


Figure 8: CAD model of a) the regular green part surface and b) the irregular green part surface

Further depicted in Figure 9 is the clear difference in the visual appearance of the surface, also based on a spherical particle model at ~ 93 % consolidation with a 3D model. While the real surface does not show the regularity as seen here, it is clear from this that a definite 'fingerprint' is formed, which depends on the processing parameters and the equipment (composite tooling) to enable the pattern to be formed. This provides some insight into surface structures and may be a precursor to structural surface creation and the functional aspect that may be enabled by such micro-processes [12].



Figure 9: The solid model of the consolidated particles shows the distinct difference in appearance

3.4 The mechanical testing

The bend samples were all tested to failure and the load data from both the radial and transverse orientations were normalised to enable comparison. The data in Figure 10 shows a 10 % average load variation between the two orientations. What it does not show, however, is whether the variation is due to the surface irregularity or some other mechanism, such as packing uniformity from a preferential flow set up during moulding. Beam theory would tend to disregard the variation created due to a surface irregularity. Considering that the load to break is a function of the depth of the section, it would take a particle deficiency of more than ten particles ($45\ \mu\text{m} \times 10$) over the section depth ($d \sim 4.60\ \text{mm}$) to create a 10 % load difference [13]. Preferential particle distribution or packing uniformity might prove a better fit to the data.

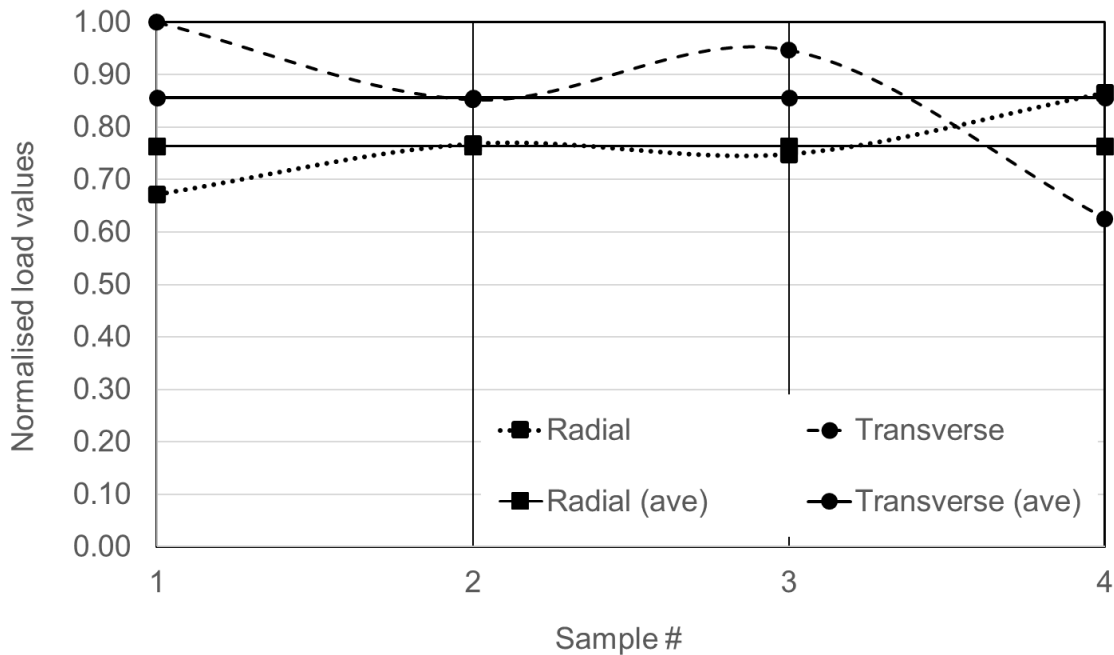


Figure 10: Normalised load values from three-point bend test of the cut Ti samples

3.5 The processed surfaces

The microscopy and mechanical testing helped confirm that the irregular surface was a defect but that it only affected the external appearance. As the outer surface of the parts would be subject to continuous environmental attack in service, it was assumed that the parts would be suitable for their intended purpose. It was also considered that, regardless of the nature and effect of the defect, it was appropriate to determine a method to improve the visual appearance. There is also evidence to suggest that surface treatment in the form of texture can also be used to improve titanium metals. This is due to the low

surface hardness, high friction coefficient, and poor abrasive wear resistance. There may also be some biological growth protection achievable through function-enabling surface engineering [14].

The first approach to modify the surface was to sand and polish, as seen in *Figure 11 b)*, which removed the irregular appearance and produced a smooth shiny face. This was followed by a grit blasting process, which provided the uniform dull matt surface shown in *Figure 11 a)*.



Figure 11: The part with processed surface: a) sanded and polished and b) bead blasted.

Secondly, bead blasting (*Figure 12 c)*) was done on the sintered surface (*Figure 12 a) & b)*). The bead blasting process was shown to produce a suitable and acceptable surface. Bead blasting produced the same result, with or without sanding and polishing, so was selected as the final process step eliminating the need for polishing. This ability to remove the irregularity caused by the particle positioning highlights the reflectivity of the titanium particles post sintering also has some part in this effect. This effect will require further investigation to fully explain.



Figure 12: The sintered part with processed surface: a) and b) the as sintered surface with different visual aspects (irregularity), c) bead blasted surface with uniform appearance

The bead blasting process used a carborundum powder with a particle size in the vicinity of 100 to 400 μm , which could have the effect of reorienting the titanium particle ($\sim 45 \mu\text{m}$) surfaces, hence the uniform appearance [15].

4 Conclusions

Using microscopic analysis it was found that the most likely mechanism for the flaw was phase separation during moulding, which produced a difference in particle distribution on the outer surface of the parts. A solid model was produced to replicate the particle deficient surface and proved a good likeness.

The irregular surface appearance was also investigated using mechanical testing. The test results proved that there was no noticeable effect on the mechanical properties when compared to a sample without the irregularity. The parts were designed to be used in the marine environment in a structural capacity. As with any structural component, product testing is best practice and used to prove the ability to perform as required. As this investigation has shown, the parts' surface post sintering did not compromise the mechanical performance and they were therefore considered to be 'fit for purpose'.

Surface treatment using bead blasting eliminated the irregular appearance, indicating that reflectivity of the titanium particles was a contributor to the visual effect.

4.1 Limitations

The investigation provides key insights into the properties and performance of the titanium structural hold down and the conclusions about it have been reached using regular experimental practice. What is also apparent is that some limitations might be addressed to improve and further substantiate the results. This includes increasing the number of samples tested in both visual and mechanical testing. Reducing subjectivity that arises from visualisation by including practices such as particulate counts and the use of other microscopy techniques such as scanning electron and digital image microscopy.

References

- [1] Oberg, E.; Jones, F.; Horton, H.; Ryffel, H.: *Machinery's Handbook* (C. McCauley (ed.); 29th ed.). Industrial Press, 2012.
- [2] German, R.; Bose, A.: *Injection Molding of Metals and Ceramics*. Metal Powder Industries Federation, 1997.
- [3] Heaney, D.: *Handbook of metal injection molding*. Woodhead Publishing, 2012.
- [4] German, Randall M.: *Sintering science: a historical perspective*. Princeton, NJ : Metal Powder Industries Federation, 2017.
- [5] Garry, M.: *Plastic and Polymer Problems? Check The Symptoms – Part 1*. ThermoFisher Scientific, 2015. <https://www.thermofisher.com/blog/materials/plastic-and-polymer-problems-check-the-symptoms-part-1/>
- [6] German, Randall M.; Bose, A.: *Binder and Polymer Assisted Powder Processing*. In: *Binder and Polymer Assisted Powder Processing*. ASM International, 2020. <https://doi.org/10.31399/asm.tb.bpapp.9781627083195>
- [7] German, R. M.: *Metal Injection Molding. A Comprehensive MIM Design Guide*. Metal Powder Industries Federation, 2011. https://www.techstreet.com/mpif/standards/metal-injection-molding-a-comprehensive-mim-design-guide?product_id=1910947
- [8] MPIF: *Standard Test Methods for Metal Powders and Powder Metallurgy Products*, (2012).
- [9] Mozetič, M.: *Surface Modification to Improve Properties of Materials*. *Materials*, 12 (2019) 3, p. 358. <https://doi.org/10.3390/ma12030441>
- [10] Ewart, P. D.; Verbeek, C. J.; Ahn, S.: *Comparative rheology techniques for assessment of MIM titanium metal powder feedstocks*. In: Tang, H.; Qian, M.; Liu, Y.; Cao, P.; Chen, G. (eds.). *Key Engineering Materials* (Vol 770). Trans Tech Publications Ltd., 2018, pp. 195–205. <https://doi.org/10.4028/www.scientific.net/KEM.770.195>
- [11] Ewart, P.: *The Formulation of Titanium-based Metal Feedstocks and the Fabrication of Parts using the Powder Injection Moulding Process*. Hamilton, New Zealand: The University of Waikato, 2015.
- [12] Tosello, G.: *Product/process fingerprint in micro manufacturing*. *Micromachines*, 10 (2019) 5, p. 3. <https://doi.org/10.3390/mi10050340>
- [13] Hibbler, R.: *Mechanics of Materials*. Pearson Education, 2018.

- [14] Lin, N.; Li, D.; Zou, J.; Xie, R.; Wang, Z.; Tang, B.: Surface texture-based surface treatments on Ti6Al4V titanium alloys for tribological and biological applications: A mini review. *Materials*, 11 (2018) 4, p. 28. <https://doi.org/10.3390/ma11040487>
- [15] Atieh, A. M.; Rawashdeh, N. A.; AlHazaa, A. N.: Evaluation of surface roughness by image processing of a shot-peened, TIG-welded aluminum 6061-T6 alloy: An experimental case study. In: *Surface Modification to Improve Properties of Materials*, 11 (2018) 5. <https://doi.org/10.3390/ma11050771>.